

Synthesis of In(Sn)-O and Sn(In)(Sb)-O System Nanoparticles Using DC Arc Plasma Method

Xie Bin, Liu Guanpeng, Li Longteng, Zhao Yanfei, Yang Shuo, Xi Yulin

Luoyang Ship Material Research Institute, Luoyang 471023, China

Abstract: A new DC arc plasma concept was proposed to produce metal oxide nanoparticles by metal melting, blasting or gasification processes. It was exemplified by the preparation of single phase nanoparticles SnO₂, In₂O₃ and SnO₂, In₂O₃-based composite nanoparticles such as In₂O₃:Sn (ITO), SnO₂:Sb (ATO) and SnO₂:In:Sb (IATO). X-ray diffraction (XRD) indicates that the doped SnO₂ and In₂O₃ are single phase and there is no other secondary phase. The results of transmission electron microscopy (TEM) show that for the prepared single phase nanoparticles with good dispersion, the particle size ranges from 20 to 50 nm. The prepared ITO and ATO nanoparticles were utilized in ITO target and ATO electrode, and their density and electrical properties were tested. The prepared ITO target and ATO electrode have high density and low resistivity, and the ITO target has good film-forming effect, which implies that the ITO and ATO nanoparticles prepared by DC arc plasma can be applied to the field of flat panel displays and conductive electrodes.

Key words: plasma; nanoparticles; metal oxide; single phase

Tin oxide (SnO₂) is an *n*-type semiconductor having a rutile crystal structure. Studies have shown that several additives (cations such as In^[1], Sb^[2], Pd^[3]...) influence the band gap of SnO₂ nanoparticles, resulting in good transparency, conductivity and high sensitivity for applications such as gas sensors, transparent conducting electrode, transistor, solar cells, special coating for energy-conversion, Li ion batteries, low-emissivity windows, and nanoelectronic devices^[4-6]. Indium oxide (In₂O₃) is a wide bandgap semiconductor ($E_g = 3.7$ eV), well-known for its useful optoelectronic properties in both doped and undoped forms^[7,8]. There are many similarities and intersections between indium oxide and tin oxide in the application of these materials^[9-11]. Thus, a great deal of research work has been devoted to the method of synthesizing SnO₂, In₂O₃ and ion-doped SnO₂ and In₂O₃ nanoparticles in a controllable manner.

Many methods have been developed to synthesis SnO₂, In₂O₃ and ion-doped SnO₂ and In₂O₃ nanoparticles, which are well known as sol-ge^[12,13], solvothermal^[14,15], chemical vapor deposition^[16,17], nonaqueous synthesis^[18],

co-precipitation^[19], and laser ablation^[20] etc. However, most investigations of the synthesis of doped and undoped SnO₂ and In₂O₃ nanoparticles have involved batch solvothermal or hydrothermal methods which are time-consuming, often requiring at least 12 h to complete and produce large amounts of residue and waste water^[21]. At the same time, hydroxides of In, Sn, Sb and Ag are also produced due to the low reaction temperature.

These nanoparticles require calcination at temperatures above 300 °C to convert to SnO₂, In₂O₃ or ion-doped SnO₂ and In₂O₃, often causing extensive particle growth or agglomeration, which may subsequently affect the overall properties of the final functional materials^[22].

In contrast to above-mentioned processes, this study provides a rapid, efficient and simpler way and uses a cost effective, environmental friendly, and convenient method to produce large scale production of SnO₂, In₂O₃, ITO, ATO and IATO powders with uniform particle size distribution, well crystallization, easy dispersion, and high purity.

1 Experiment

Received date: July 15, 2017

Foundation item: the Chinese National Major Special Project for the Rare Earth and Rare Metallic Materials (20121743)

Corresponding author: Xi Yulin, Ph. D., Researcher, Luoyang Ship Material Research Institute, Luoyang 471023, P. R. China, Tel: 0086-379-67256129, E-mail: xiylun@725.com.cn

Copyright © 2018, Northwest Institute for Nonferrous Metal Research. Published by Elsevier BV. All rights reserved.

Fig.1 illustrates the DC arc plasma synthesis procedure for the production of nanoparticles. In our synthesis experiment, the key part shown in Fig.1 is a special and unobtrusive DC arc plasma reactor, which is connected to an AC generator with a maximum power of 300 kW and using about 245 kW of power. The reaction chamber was evacuated to 0.01 MPa and the dried and cooled air was filled with plasma gas. As for raw materials preparation, the purity > 99.99% of Sn, In ingots and InSn, SbSn, InSbSn alloy ingots (mass ratios of the raw materials are shown in Table 1) were heated to their melting points. Next, as-prepared precursors were injected into the water cooled plasma reactor. The molten raw materials can be immediately evaporated due to the high temperature of the thermal plasma, and the metal vapor is oxidized at the same time. A larger temperature gradient can be formed on the shell of the reactor by the cooling water circulation system, which facilitates crystallization. Finally, the formed nano-oxide particles escaped from the reactor chamber along with the cooled air.

The phase formation of the obtained SnO₂, In₂O₃, ITO, ATO, and IATO nanoparticles was verified by X-ray diffractometer (XRD, DMAX 2500, Rigaku Co.) The morphology

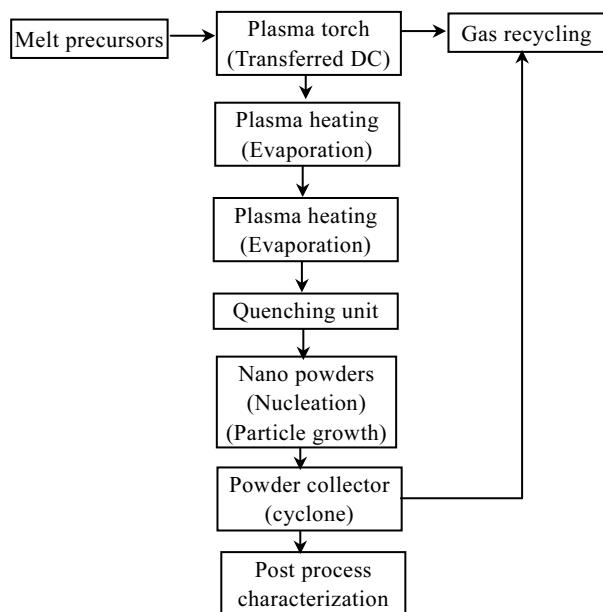


Fig.1 Synthesis procedure of nanoparticles by DC arc plasma

Table 1 Mass ratio of raw materials (wt%)

Sample No.	In	Sn	Sb
1	0	100	0
2	0	99	1
3	5	90	5
4	100	0	0
5	90	10	0

and particle size of the obtained particles were analyzed by transmission electron microscopy (TEM, JEM-2100F, Jeol Co.) Additionally, the prepared ITO and ATO sample were prepared as ITO target and SnO₂-based ceramic electrode sample, respectively (Cylinder diameter $\Phi=100$ mm and thickness about 10mm), and then the density and resistivity were measured by standard Archimedes method and four-probe method, respectively (MCP-T600, Mitsubishi Chemical). Scanning electron microscope (SEM, JEOL JSM-6400) was used to observe the morphology of the ITO target and the SnO₂ based ceramic electrode.

2 Results and Discussion

Fig.2 shows the XRD patterns of the synthesized SnO₂, ATO, IATO, In₂O₃, ITO nanoparticles. The XRD patterns of samples exhibit sharp diffraction peaks, which indicate a good crystallinity of the samples. The peaks of sample 2 and sample 3 display tetragonal rutile tin oxide as sample 1 (PDF#70-4177) and no indium, antimony or their oxide peaks were observed. Similarly, sample 5 still keeps the bixbite crystal structure just as sample 4(PDF#71-2195). There is no diffraction peak of tin or tin oxide, suggesting that the doped cations were completely solvated in the parent phase. In this work, undoped SnO₂ and In₂O₃ were referred as pure and used as control samples. It is clear between sample 1 and sample 2 that the 2θ of (110) plane changes from 26.75° in sample 1 to 26.50° in sample 2. The (101), (211) planes of sample 2 and sample 3 also shift to a lower angles relative to sample 1. In sample 2 and sample 3, the peak broadening was observed. J. Rockenberger et al^[23] reported that doping antimony into tin oxide and doping tin into indium oxide induces some changes in the diffraction pattern: the width of the peak increases and the location of the peak moves to lower angles. The ionic radius of antimony is 0.076 nm, which is larger than that of tin ($r=0.069$ nm). The unit cell volume of tin oxide increases with Sb³⁺ doping^[24]. It is also clear between sample 4 and sample 5 that the 2θ of (222), (400), (440) and (622) planes of sample 5 moves to a lower angles relative to sample 4. It is unable to explain this phenomenon by Bragg equation and the theory of quantum chemistry. The ionic radius of tin is 0.069 nm, which is smaller than that of indium ($r=0.094$ nm). With the increase of doping content, the diffraction angle should be shifted to high angle instead of low angle, and the unit cell volume should be decreased rather than increased. The above abnormal phenomenon appears because no new compound is formed with the doping of Sn⁴⁺, while the lattice distortion is caused by the substitution of In³⁺, and the ionic radius of Sn⁴⁺ is smaller than that of In³⁺, resulting in residual stress during the crystallization process. In addition, the repulsion between the excess positive charge of Sn⁴⁺ may create extra swelling in the rhombohedral structure^[25].

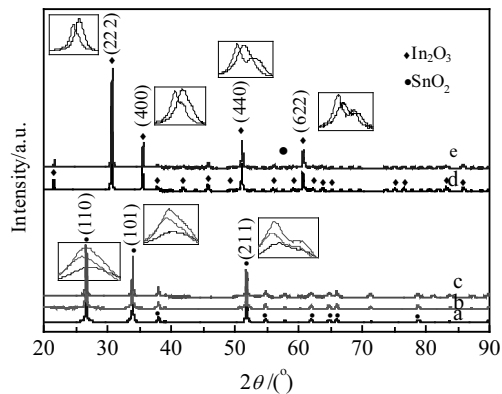


Fig.2 XRD patterns of the synthesized nanoparticles (a-sample 1, b-sample 2, c-sample 3, d-sample 4, and e-sample 5)

The prepared SnO_2 , In_2O_3 , ITO, ATO, and IATO nanoparticles were characterized by TEM, the images are shown in Fig.3. The nanoparticles were well-defined, and most of which are spherical (sample 1, 2, 3, 5) and cubical (sample 4) with a size in the range of 20~50 nm, indicating that the prepared nanoparticles have good dispersibility and no agglomeration. The size of the ITO nanoparticles prepared by the DC arc plasma method is smaller and more

uniform than those in Fig.3a~3d.

In order to study the properties of ITO and ATO powders prepared by DC arc plasma, these two kinds of powders were prepared as ITO target and SnO_2 ceramic electrode. Firstly, a high solid content ITO slurry was prepared after the powder ball milling and granulating. Then the ITO slurry was put into a ceramic green body by slip casting. Finally, the ITO target was prepared after the degreasing and sintering process of the ceramic green body. The process of preparing SnO_2 ceramic electrode is similar to the ITO target prepared in the present study. The difference is that the ATO nanoparticles used are doped with 1% ZnO and the particle size is about 50 nm.

Fig.4a shows the SEM images of the ITO target, it is found that ITO target prepared by DC arc plasma is very dense and the grain size is relatively small. Numerous small grains exist near the grain boundary, which are all secondary phases $\text{In}_4\text{Sn}_3\text{O}_{12}$ ^[26]. Additionally, the ITO thin film sample was synthesized by DC magnetron sputtering, and the prepared ITO target was used as a sputtering source. Fig.4b shows the optical properties of ITO thin films, the transmittance of ITO thin films deposited under the conditions (Table 2) is over 85%. The results (Table 2 and Fig.4b) of the ITO thin film sample shows that the film has good optical and electrical properties, indicating that the ITO nanoparticles synthesized by the DC arc plasma method can be used for the preparation of ITO targets, and

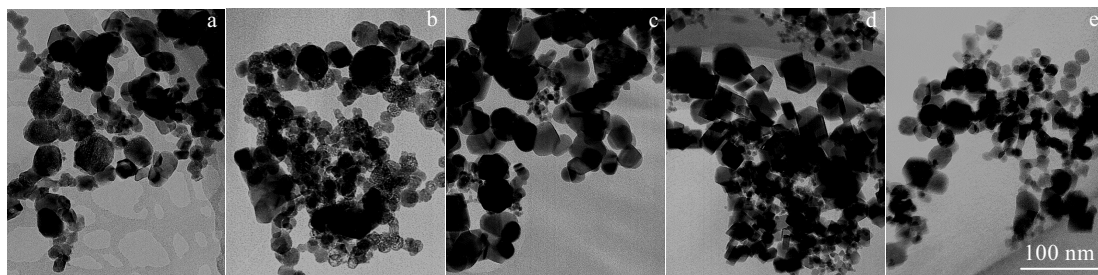


Fig.3 TEM images of the synthesized nanoparticles: (a) sample 1, (b) sample 2, (c) sample 3, (d) sample 4, and (e) sample 5

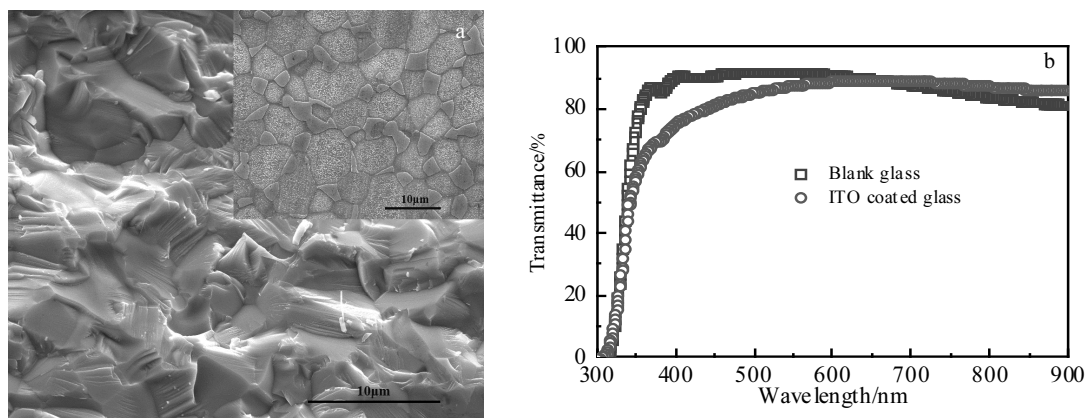


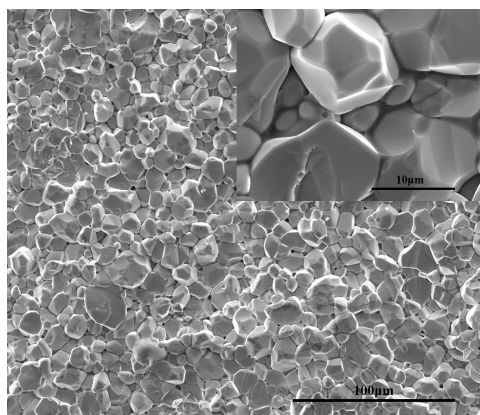
Fig.4 SEM images of the ITO target (a) and optical transmittance of the film (b)

Table 2 Preparation conditions and properties of the ITO thin film sample

Preparation conditions				Properties			
Sputtering Temperature/°C	Argon-oxygen flow ratio	Working pressure/Pa	Power density/W·cm ⁻²	Thickness/nm	Resistivity/ $\times 10^{-4} \Omega \cdot \text{cm}$	Carrier concentration, N/cm^{-3}	Carrier mobility, $\mu_{\text{H}}/\text{cm}^2 \cdot \text{V}^{-1} \cdot \text{s}^{-1}$
350	0.6/40	0.4	0.68	21.5	1.63	1.32×10^{21}	32.6

the various properties of the film meets the requirements of flat panel displays.

Fig.5 shows the SEM images of SnO₂ ceramic electrode. Grains on the cross section of the electrode tend to be smooth and arranged densely; voids within the grains are filled with small particles of doped ZnO. The doped ZnO in the parent phase is uniform and there is no segregation. Density and resistivity tests show that the density and resistivity of the prepared SnO₂ electrode are 6.62 g/cm³ and 88 $\Omega \cdot \text{cm}$, respectively.

Fig.5 SEM images of prepared SnO₂ electrode

3 Conclusions

1) We have demonstrated a facile strategy for fast formation of single phase and doped metal oxides nanoparticles with uniform morphology and sizes of 20~50 nm.

2) ITO and ATO nanoparticles prepared by DC arc plasma were utilized in ITO target and SnO₂ electrode, which have high density and low resistivity and can be applied to the field of flat panel displays and conductive electrodes.

References

- Carreri F C, Sabelfeld A, Gerdes H et al. *Surface and Coatings Technology*[J], 2016, 290: 65
- Esro M, Georgakopoulos S, Lu H, Vourlias G et al. *Journal of Materials Chemistry C*[J], 2016, 4(16): 3563
- Wang Q J, Wang C, Sun H B et al. *Sensors and Actuators B: Chemical*[J], 2016, 222: 257
- Tomer V K, Duhan S. *Sensors and Actuators B: Chemical*[J], 2016, 223: 750
- Mueller F, Bresser D, Chakravadhanula V S K et al. *Journal of Power Sources*[J], 2015, 299: 398
- Shao Tingting, Zhang Chunfu, Zhang Weihu. *Rare Metal Materials and Engineering*[J], 2015, 44(10): 2409 (in Chinese)
- Hafeezullah, Yamani Z H, Iqbal J et al. *Journal of Alloy and Compounds*[J], 2014, 616: 76
- Regoutz A, Egdell R G, Morgan D J et al. *Applied Surface Science*[J], 2015, 349: 970
- Ma Xiaobo, Zhang Weijia, Wang Dongxin et al. *Rare Metal Materials and Engineering*[J], 2015, 44(12): 2937 (in Chinese)
- Ellmer K. *Nature Photonics*[J], 2012, 6: 809
- Tang W, Wang Y Q, Liu J et al. *Rare Metal Materials and Engineering*[J], 2015, 44(11): 2683
- Aziz M, Abbas S S, Baharom W R W. *Materials Letters*[J], 2013, 91: 31
- Köse H, Karaal Ş, Aydin A O et al. *Materials Science in Semiconductor Processing*[J], 2015, 38: 404
- Gu Y Y, Qin L P. *Rare Metals*[J], 2008, 27(1): 27
- Lin L T, Tang L, Zhang R et al. *Materials Research Bulletin*[J], 2015, 64: 139
- Wang C Y, Ali M, Kups T et al. *Sensors and Actuators B: Chemical*[J], 2008, 130(2): 589
- Vomiero A, Ferroni M, Natile M M et al. *Applied Surface Science*[J], 2014, 323: 59
- Neri G, Bonavita A, Micali G et al. *Sensors and Actuators B: Chemical*[J], 2008, 130(1): 222
- Kanoksinwuttipong J, Pecharapa W, Noonuruk R et al. *Key Engineering Materials*[J], 2015, 659: 604
- Donato N, Neri F, Neri G et al. *Thin Solid Films*[J], 2011, 520(3): 922
- Elouali S, Bloor L G, Binions R et al. *Langmuir*[J], 2012, 28: 1879
- Pantilimon M C, Tea S K, Lee S J. *Ceramics International*[J], 2015, 42(3): 3762
- Rockenberger J, Zum Felde U, Tischer M et al. *Journal of Chemical Physics*[J], 2000, 112(9): 4296

- 24 Zhang J R, Gao L. *Materials Chemistry and Physics*[J], 2004, 87(1): 10
25 González G B, Cohen J B, Hwang J H et al. *Journal of Applied Physics*[J], 2001, 89(5): 2550
26 Kim S M, Seo K H, Lee J H et al. *Journal of the European Ceramic Society*[J], 2006, 26(1-2): 73

直流电弧等离子体法制备 In(Sn)-O 及 Sn(In)(Sb)-O 系纳米颗粒

谢 斌, 刘冠鹏, 李龙腾, 赵延飞, 杨 硕, 郝雨林
(中国船舶重工集团公司第七二五研究所, 河南 洛阳 471023)

摘 要: 采用一种新的直流电弧等离子体法, 通过对熔融的金属进行爆破(或气化), 制备出了单相 SnO₂、In₂O₃ 纳米颗粒以及 In₂O₃:Sn (ITO)、SnO₂:Sb (ATO)和 SnO₂:In:Sb (IATO)多元复合纳米颗粒。XRD 结果表明, 所制备的 SnO₂ 和 In₂O₃ 基多元复合纳米颗粒均为单相结构, 没有其它杂相; TEM 结果表明, 直流电弧等离子体所制备的单相纳米颗粒分散性好, 尺寸 20~50 nm。该法合成的纳米 ITO 和 ATO 颗粒所制备的 ITO 靶材和 SnO₂ 电极密度高、电阻率低, 表明所制备的 ITO 和 ATO 纳米颗粒可以应用于平板显示和导电电极领域。

关键词: 等离子体; 纳米粉体; 金属氧化物; 单相结构

作者简介: 谢 斌, 男, 1986年生, 硕士, 中国船舶重工集团公司第七二五研究所, 河南 洛阳 471023, 电话: 0379-67256240, E-mail: xiebin@725.com.cn